Edwards's statistical mechanics of crumpling networks in crushed self-avoiding sheets with finite bending rigidity

Alexander S. Balankin and Leonardo Flores-Cano
Grupo "Mecánica Fractal," ESIME-Zacatenco, Instituto Politécnico Nacional, México D.F. 07738, Mexico
(Received 28 April 2014; revised manuscript received 16 January 2015; published 5 March 2015)

This paper is devoted to the crumpling of thin matter. The Edwards-like statistical mechanics of crumpling networks in a crushed self-avoiding sheet with finite bending rigidity is developed. The statistical distribution of crease lengths is derived. The relationship between sheet packing density and hydrostatic pressure is established. The entropic contribution to the crumpling network rigidity is outlined. The effects of plastic deformations and sheet self-contacts on crumpling mechanics are discussed. Theoretical predictions are in good agreement with available experimental data and results of numerical simulations. Thus, the findings of this work provide further insight into the physics of crumpling and mechanical properties of crumpled soft matter.

DOI: 10.1103/PhysRevE.91.032109 PACS number(s): 62.20.F−, 87.16.dm, 89.75.Da

I. INTRODUCTION

Crumpling of thin matter is ubiquitous in both nature and engineering, starting from folding of graphene nanosheets [1] to geological formations [2]. Accordingly, crumpling phenomena have attracted much interest in science and technology [3–5]. A remarkable characteristic of thin materials is that their bending rigidity is much lower than the stretching one. For this reason, the curvature imposed on a thin sheet is concentrated in sharp creases and developable cones, whereas a major fraction of sheet area remains relatively flat and unstrained [6–8]. Under increasing confinement of crushed sheet the crumpling creases asymptote to almost linear ridges which meet at pointlike vertices and form a branched crumpling network accumulating a major part of deformation energy [9–11]. Consequently, the crumpling behavior of self-avoiding sheets with finite bending rigidity is governed by an evolving network of crumpling ridges. This is reflected in anomalously large resistance of folded sheets to hydrostatic compression [12–15], whereas their resistance to shear and axial loads is quite low [15–20].

Another noteworthy feature of crumpling networks in randomly crushed thin sheets is their statistical scale invariance within a wide range of length scales [21,22]. This gives rise to the fractal geometry of both a crumpled sheet configuration [22–26] and a set of balls folded from sheets of different sizes under the same confinement force [1,13,14,20,27–31]. The relationships between the fractal dimensions of a crumpling network and sheet configuration were established in Ref. [22]. In this context, it is pertinent to point out that the fractal dimensions of ball configuration and the fractal dimension of a set of balls folded by the same forces are generally different due to elastic strain relaxation after the confinement force is withdrawn [23]. It was also recognized that both fractal dimensions are independent of the sheet elastic properties [20–30], but may change due to plastic deformations of the sheet material [26,28,31]. Consequently, although the crumpling processes appear quite haphazard, the crumpling behavior is well defined in a statistical sense and rather well reproducible in experiments [13–20,32]. Moreover, almost all thin materials display nearly the same scale invariant crumpling behavior [22]. This has allowed the authors of Ref. [28] to model graphene-based nanosheets crumpled by capillary forces with the help of relations established in Ref. [13] for randomly folded aluminum foils. Furthermore, acoustic emission from hand crushed paper reproduces some essential attributes of seismic events [33]. Therefore, a better understanding of crumpling processes in simple model systems has tremendous importance from the fundamental and applied standpoints.

The crumpling behavior of thin sheets is strongly dependent on the confinement mode [15,22] and sheet geometry [22,34]. One of the basic modes is the crumpling of a thin sheet subjected to isotropic confinement [22,29–31,35]. Under increasing hydrostatic pressure (P) an initially flat square sheet is folded into an approximately spherical ball of diameter R with the packing density

$$\rho = \frac{6hL^2}{\pi R^3} \leqslant 1, \tag{1}$$

where h and L are the sheet thickness and edge size, respectively. As the compaction ratio $K = L/R$ increases, the packing density increases up to $\rho = 1$ at $K_{\max} = (\pi L/6h)^{1/3}$. Experiments [12–15], theoretical considerations [9–13,15,22,28,36], and numerical simulations [29–31,35,36,37] suggest that once K exceeds the threshold value K_{th} ($K_{\text{th}} \approx 1.7$ [29,30]) the sheet packing density exhibits a power-law dependence on P. That is,

$$\rho = AP^{1/\eta}, \tag{2}$$

where A is the material-dependent constant, whereas the scaling exponent $\eta \geqslant 2$ [22]. In the case of linearly elastic self-avoiding sheets with finite bending rigidity, numerical simulations [29–31] and theoretical arguments [22] suggest that the scaling exponent $\eta = 2$ is universal. Plastic deformations and friction were considered as possible origins for effective softness of crumpled materials [13,14,31]. The increase of η for elastoplastic sheets was observed in experiments [14] and further reproduced by numerical simulations [31]. Furthermore, more recent experiments [38] and molecular dynamics simulations [37,39] reveal that isotropically confined self-avoiding sheets obey the scaling behavior (2) only within a bounded range of packing density,

$$\rho_{\text{th}} = 6hK_{\text{th}}^3/\pi L \leqslant \rho \leqslant \rho_1 \approx 0.5, \tag{3}$$

whereas at larger ρ the rate $\partial\rho/\partial P$ decreases almost exponentially. In Ref. [29] the change in the functional dependence of $\rho(P)$ was attributed to the effect of sheet self-contacts at high packing density. Further, in Ref. [38] the increase of $\partial\rho/\partial P$ was linked with the appearance of long-range correlations in the cluster structure of a crumpled sheet (see Ref. [26]). Based on this finding, the authors of Ref. [38] have proposed the mechanical bundled-layer model which provides a good fit to experimental pressure-packing density behavior without an account for the contribution of sheet self-contacts.

At the same time, in numerical simulations [30] and experiments [40] it was observed that under increasing external confinement the configuration of the crumpling network evolves to a state with either minimum elastic energy or maximum entropy. Hence, one might expect that the mechanical response of randomly crumpled sheets can be explained within a framework of the Edwards's statistical mechanics of crumpling networks (see Refs. [17,19,41,42]). Although the Edwards's statistical mechanics was originally developed to deal with granular matter and spin glasses [42,43], its applicability to cellular systems and crumpling networks with jammed states has been already discussed in Refs. [17,18,41,42,44].

In this paper, the Edwards-like statistical mechanics of crumpling networks is developed and the statistical distribution of ridge lengths in a self-avoiding sheet with finite bending rigidity is derived. This allows us to establish the relationship between the sheet packing density and hydrostatic pressure. The paper is organized as follows. In Sec. II the scaling properties of crumpling ridges and crumpling networks are outlined. The minimum and maximum ridge lengths and the total number of ridges in a sheet crushed into a spherical ball are deduced. Section III is devoted to the Edwards-like statistical mechanics of crumpled sheets. The ridge length distribution is established and thermodynamic potentials of a crumpling network are defined. The pressure-packing density relationship is derived in Sec. IV. Some relevant conclusions are outlined in Sec. V.

II. CHARACTERISTIC FEATURES OF CRUMPLING RIDGES AND A CRUMPLING NETWORK

When a thin sheet is confined to a ball of diameter R much smaller than the sheet size L (see Fig. 1) nearly all the deformation energy is concentrated in a network of almost straight ridges that meet at sharp vertices. The boundary-layer analysis of the ridge singularity in a thin plate suggests that the width of a crumpling ridge (w) is related to its length (l) as

$$w = l^{2/3}(\kappa/Y_2)^{1/6}, \tag{4}$$

where κ and Y_2 are the effective bending and stretching moduli of sheet [6]. Both moduli of an elastic sheet are dependent on the sheet thickness h [45,46], whereas the apparent stretching modulus of an elastoplastic sheet is thickness independent [34,47]. Specifically, the effective bending and stretching moduli of elastic and elastoplastic sheets are equal to

$$\kappa = \frac{Y_2 h^2}{12(1-\mu^2)} = \frac{Y_3 h^3}{12(1-\mu^2)} \propto h^3 \quad \text{and} \quad \kappa = \frac{Y_2 h^2}{9} \propto h^2, \tag{5}$$

FIG. 1. Illustration of the definition of vectors $\vec{r}_{i1}$, $\vec{r}_{i2}$, and $\vec{l}_i$ in the crumpling network of a folded sheet.

respectively, where γ_3 is the three-dimensional Young modulus and μ is the Poisson ratio of the sheet material [46,47].

The solution of von Kármán equations suggests that the elastic energy stored in the crumpling ridge consists of similar amounts of bending (ε_b) and stretching (ε_s) energy and depends on the ridge length l as

$$\varepsilon \approx \kappa(l/h)^{1/3}, \tag{6}$$

whereas the ratio of the bending and stretching energies stored in the ridge is determined by the virial theorem [6b]. For sheets with larger dimensionless Föppl–von Kármán number $\chi = (L/h)^2 \gg 1$ and $l \gg h$, the ratio $\varepsilon_b/\varepsilon_s$ has been predicted to have the universal value of $\varepsilon_b/\varepsilon_s = 5$ [6b].

In a thin sheet confined into a ball the lengths of crumpling ridges vary in the interval of $l_{\min} \leqslant l \leqslant l_{\max}$, where $l_{\min}$ and $l_{\max}$ are the minimum and maximum ridge lengths [48–50]. Furthermore, it is easy to understand that the minimum width of a crumpling ridge in a confined sheet is $w_{\min} = \pi h$. Therefore, from Eqs. (4) and (5) it follows that the minimum ridge length is equal to

$$l_{\min} = [12\pi^6(1-\mu^2)]^{1/4} h = \omega h, \tag{7}$$

where the constant ω varies from 10.4, if $\mu = 0$, to 9.6, if $\mu = 0.5$, whereas for elastoplastic sheets $\omega = 9.6$. Notice that Eq. (7) is consistent with the results of experimental studies [17,21,22,40,48–50] and molecular dynamics simulations [29–31,37].

On the other hand, it is easy to understand that the maximum ridge length is always less than or equal to the folded ball diameter. Furthermore, it is a straightforward matter to deduce that in the limit of $\rho \to 1$ the width of all ridges is equal to $w_{\min} = \pi h$ and so $l_{\max} \to l_{\min}$. Consequently, in this limit, the total number of ridges is expected to be equal to

$$N_0 = \frac{L^2}{w_{\min} l_{\min}} = \frac{1}{\pi\omega}\left(\frac{L}{h}\right)^2 \approx 0.03\chi. \tag{8}$$

The scale invariance of crumpling networks implies that under increasing isotropic confinement $K \geqslant K_{\text{th}}$ the total number of ridges scales with the sheet packing density (1) as

$$\overline{N} = N_0 \rho^{\alpha}, \tag{9}$$

where the overline denotes the ensemble average and α is the material-dependent exponent, while the packing density $\rho_{\text{th}} \leqslant \rho \leqslant 1$. The statistical scaling invariance of the crumpling network also leads to the scaling relation $\overline{N} \propto l_{\max}^{D_2}$, where D_2 is the fractal dimension of the crumpling network impression on the unfolded sheet [22]. Therefore, one can expect that the ratio $l_{\max}/l_{\min}$ scales with the packing density (1) as

$$l_{\max}/l_{\min} = (\overline{N}/N_0)^{1/D_2} = \rho^{-\varphi}, \tag{10}$$

where $\varphi = \alpha/D_2$. However, questions about the crumpling ridge length distribution and, consequently, its effect on the crumpling mechanics remain still open (see discussion in Refs. [3,17–19,21,22,29–31,37,41,48–51,52]). The gamma distribution is commonly used to fit the crumpling length distributions obtained either in experiments [17,21] or by numerical simulations [48]. Alternatively, a log-normal distribution was also suggested to represent the statistical distribution of crumpling ridge lengths [3,29,48]. Besides, some other statistical distributions were used to fit specific data sets (see Refs. [50,51]). In this regard, in view of a crumpling network self-similarity, we can assume that in an isotropically confined sheet the ratio of distribution mode (l_{mod}) to the maximum ridge length is independent of packing density. That is, in a thin sheet crumpled under isotropic confinement,

$$l_{\max}/l_{\text{mod}} = k, \tag{11}$$

where k can be a function of the Föppl–von Kármán number χ. Furthermore, it was shown that the fractal dimension of a crumpling network in the folded state (D) is related to the fractal dimension D_2 as

$$D = D_2 D_b/2, \tag{12}$$

where D_b is fractal dimension of ball configuration [22]. For a given confinement mode (e.g., axial, radial, and isotropic compression, or hand crumpling [22]) of purely elastic sheets the fractal dimensions D_2, D_b, D, and the scaling exponent α are expected to be material independent. Specifically, for isotropically confined purely elastic self-avoiding sheets, it was suggested that $D_2 = 11/6$, $D_b = 8/3$, $D = 22/9$, and $\alpha = 11/9$ [22], and so $\varphi = 2/3$. This is consistent with the results of numerical simulations in which it was found that $1.13 \leqslant \alpha \leqslant 1.33$ [29,31] and so, numerically, $\varphi = \alpha/D_2 = 0.67 \pm 0.06$.

III. STATISTICAL MECHANICS OF CRUMPLING NETWORKS

As a thin sheet is confined, the configuration of the crumpling network changes due to sudden buckling of existing and formation of new crumpling ridges [6,17,40,53]. In this regard, it was found that the energy of a ridge can change by no more than a finite fraction before it buckles [6b]. So, the crumpling process can be viewed as a stepwise sequence of nonequilibrium jammed states of the crumpling network. Furthermore, it was shown that in a crumpled sheet two ridges with comparable lengths and dihedral angles have comparable energies, even though they have different loads [6b]. Therefore, a jammed state of a crumpling network can be completely defined by a set of vectors $\{\vec{r}_{ij}\}$ pointing to each end of every ridge, where $i = 1,2,\ldots,N$ counts the ridges ($N \leqslant N_0$), while $j = 1,2$ enumerates extremes of each ridge (see Fig. 1). This allows us to construct the Edwards-like statistical mechanics of evolving crumpling networks.

The Edwards's approach (see Refs. [42–44]) may be summarized as follows. For a given configuration attained dynamically, physical observables can be obtained by averaging over the usual equilibrium distribution at the corresponding volume, energy, etc., but restricting the sum to inherent states defined as the stable configurations in the potential energy landscape. The strong ergodic hypothesis that all jammed configurations of a given volume can be taken to have equal statistical probabilities leads to definition of the configurational entropy (S) as the logarithm of the number of jammed configurations with a given number of ridges (N), volume (V), and energy (E). Specifically, the configurational entropy of crumpling networks can be defined in a straightforward manner as

$$S(p) = -\int d\mu\{r_{ij}\} p\{r_{ij}\} \ln p\{r_{ij}\}, \tag{13}$$

where $p\{r_{ij}\}$ is the probability density of network configuration $\{\vec{r}_{ij}\}$ and $d\mu\{\vec{r}_{ij}\}$ is the volume element in a fractal configuration space, such that

$$\int d\mu\{\vec{r}_{ij}\} p\{\vec{r}_{ij}\} = 1 \tag{14}$$

whereas the mean total number and length of all ridges in the crumpling network are equal to

$$\begin{aligned} \overline{N} &= \int d\mu\{\vec{r}_{ij}\} p\{\vec{r}_{ij}\} \aleph\{\vec{r}_{ij}\} \quad \text{and} \\ \Lambda &= \int d\mu\{\vec{r}_{ij}\} p\{\vec{r}_{ij}\} \ell\{\vec{r}_{ij}\}, \end{aligned} \tag{15}$$

respectively, where $\aleph\{\vec{r}_{ij}\}$ and $\ell\{r_{ij}\} = \sum_{i=1}^{\aleph} |\vec{r}_{i2} - \vec{r}_{i1}|$ are the number of ridges and the sum of ridge lengths for a given configuration of the crumpling network.

The maximization of entropy (13) leads to

$$p(\ell\{\vec{r}_{ij}\}, \aleph\{\vec{r}_{ij}\}) = \frac{1}{Z} \exp(-\beta \ell\{\vec{r}_{ij}\} - \zeta \aleph\{\vec{r}_{ij}\}), \tag{16}$$

where Z is the partition function that normalizes $p(\ell,\aleph)$, whereas the Lagrange multipliers β and ζ play the role of the inverse effective temperature and external force, respectively.

A. Statistical distribution of ridge lengths in a crumpling network

The marginal probability density function of ridge length can be calculated in a straightforward way as follows:

$$\begin{aligned} p(l) &= \int d\mu\, p(\ell\{\vec{r}_{ij}\}, \aleph\{\vec{r}_{ij}\}) \\ &= \frac{1}{Z} \int d\mu \exp(-\beta\ell - \zeta\aleph) \times \delta(l - |\vec{r}_{k2} - \vec{r}_{k1}|) \\ &\quad \times \int dN \delta(N - \aleph) \end{aligned}$$

$$= \frac{1}{Z}\int d\mu \exp(-\zeta\aleph) \times \exp(-\beta\ell)\,\delta(N-\aleph) \times \delta(l-|\vec{r}_{k2}-\vec{r}_{k1}|) = \frac{1}{Z}\int dN \exp(-\zeta N)\Phi(l,N), \quad (17)$$

where the delta function $\delta(l-|\vec{r}_{k2}-\vec{r}_{k1}|)$ accounts for the sheet self-avoidance, whereas $\delta(N-\aleph)$ restricts the configurational space $\{\vec{r}_{ij}\}$ to the space $\{\vec{r}_{ij}\}_N$ with exactly N ridges, while

$$\Phi(l,N)=\int d\mu\{\vec{r}_{ij}\}_N \exp(-\beta\ell\{\vec{r}_{ij}\}_N)\delta(l-|\vec{r}_{k2}-\vec{r}_{k1}|) \quad (18)$$

is the marginal counting integral. Following to Refs. [43,44], integral (18) can be presented in the following form:

$$\Phi(l,N) = \frac{1}{N!}\int\prod_{i=1}^{N} d\mu(\vec{r}_{i2},\vec{r}_{i1})\Psi\{\vec{r}_{ij}\}_N \times \exp(-\beta\ell\{\vec{r}_{ij}\}_N)\delta(l-|\vec{r}_{k2}-\vec{r}_{k1}|) = \frac{1}{N!}\int\prod_{i=1}^{N} d\mu(\vec{r}_{i1})d\mu(\vec{l}_i)\Psi(\{\vec{r}_{i1},\vec{l}_i\}_N) \times \exp\left(-\beta\sum_{j=1}^{N} l_j\right)\delta(l-l_k), \quad (19)$$

where $d\mu\{\vec{r}_{ij}\} = \prod_{i=1}^{N} d\mu\{\vec{r}_{i2},\vec{r}_{i1}\}/N!$, $\vec{l}_i = \vec{r}_{i2}-\vec{r}_{i1}$, $l_i = |\vec{l}_i|$, $\ell\{\vec{r}_{ij}\} = \sum_{i=1}^{N} l_i$, and

$$d\mu\{\vec{r}_{i1},\vec{r}_{i2}\} = d\mu(\vec{r}_{i1})d\mu(l_i), \quad (20)$$

while $\Psi(\{\vec{r}_{i1},\vec{l}_i\}_N) = \prod_i^N \Theta(l_i-l_{\min})\Theta(l_{\max}-l_i)$ is a constraint function restricting the integral to the ensemble of admissible configurations of the crumpling network with $l_{\min}\leqslant l_i\leqslant l_{\max}$, and $\Theta(\cdots)$ denotes the step function.

Taking into account the scale invariance of crumpling network, the fractional volume element (20) can be presented in spherical coordinates as $d\mu = d\mu(l_i)d\mu(\vec{r}_{i1})$, where $d\mu(l_i) = l_i^{D-1}dl_i$ and $d\mu(\vec{r}_{i1}) = d\Omega^{D-1}$ [54], while $2<D<3$ is the fractal dimension of the crumpling network (12). Accordingly, the marginal counting integral (19) takes the following form:

$$\Phi(l,N) = \frac{V_D I^{N-1}}{N!}\exp(-l)\,l^{D-1}, \quad (21)$$

where $V_D = \int d\mu\{\vec{r}_{ij}\}$ and $I = \int d\mu(\vec{l})\Theta(l_{\min}-l)\Theta(l-l_{\max})\exp(-\beta l)$. Consequently, after the substitution of Eq. (21) into Eq. (17) and application of the normalization condition

$$\int_{l_{\min}}^{l_{\max}} p(l)dl = 1, \quad (22)$$

we get the statistical distribution function of ridge lengths in the following form:

$$p(l) = \begin{cases} \dfrac{\beta^D l^{D-1}\exp(-\beta l)}{\gamma(D,\beta l_{\min},\beta l_{\max})}, & \text{if } l_{\min}\leqslant l\leqslant l_{\max} \\ 0, & \text{otherwise} \end{cases}, \quad (23)$$

where $\gamma(s;x_1,x_2) = \int_{x_1}^{x_2} t^{s-1}e^{-t}dt = \Gamma(s;x_1)-\Gamma(s;x_2)$ is the generalized incomplete gamma function, while $\Gamma(s;x_i)$ is the upper incomplete gamma function.

The mode of distribution (23) is $l_{\,\mathrm{mod}} = (D-1)/\beta$. Accordingly, using relations (10) and (11), the generalized effective temperature of the crumpling network can be expressed as the function of packing density (1) as

$$\beta^{-1} = \frac{l_{\,\mathrm{mod}}}{D-1} = \frac{l_{\max}}{a} = ch\rho^{-\varphi}, \quad (24)$$

where coefficients

$$a = (D-1)l_{\max}/l_{\,\mathrm{mod}} \quad (25)$$

and $c=\omega/a$ can be functions of the Föppl–von Kármán number χ, sheet geometry, and confinement mode. Notice that for purely elastic self-avoiding sheets $\varphi = 2/3$ and so $\beta\propto\rho^{2/3}\propto K^2$.

The mean ridge length in the crumpling network obeying the statistical distribution (23) decreases with increase of β as

$$\langle l\rangle = \int_{l_{\min}}^{l_{\max}} lp(l)dl = \frac{\gamma(D+1;\beta l_{\min},a)}{\gamma(D;\beta l_{\min},a)}\beta^{-1}, \quad (26)$$

where $l_{\min}$, $l_{\max}$, β, and a are defined by Eqs. (7), (10), (24), and (25), respectively. Figure 2 shows the graphs of $\beta\langle l\rangle$ versus $\beta l_{\max}$ for different $\beta l_{\min}$. One can see that in the limit of low compactivity ($\beta l_{\max}\to\infty$) the mean ridge length depends on the generalized effective temperature as

$$\langle l\rangle = l_{\min} + D\beta^{-1}, \quad (27)$$

whereas in the limit of high packing density ($\rho\to 1$) the mean ridge length $\langle l\rangle \to l_{\,\mathrm{mod}} \to l_{\max}\to l_{\min}$. Figures 2 and 3 show the graphs of the probability density distribution (23) along with the conventional gamma distribution. It is instructive to note that in the limit of $\beta l_{\max}\to\infty$ the statistical distribution (23) is converted into the conventional shifted

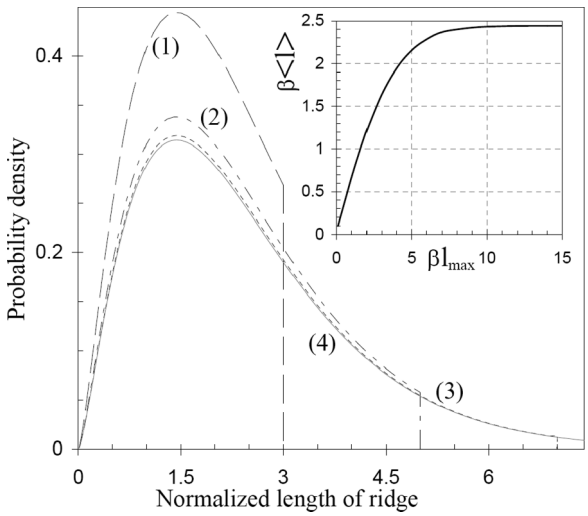

FIG. 2. Probability density distribution (23) of normalized ridge length βl in crumpling networks the same $D = 22/9 = 2.44$, $\beta l_{\min} = 0.1$, and mode $\beta l_{\,\mathrm{mod}} = (D-1) = 1.44$, but different maximum ridge length $\beta l_{\max} = 3\,(1), 5\,(2), 10\,(3)$, and the gamma distribution (4). Inset shows the graph of normalized ridge length $\beta\langle l\rangle$ versus $\beta l_{\max}$.

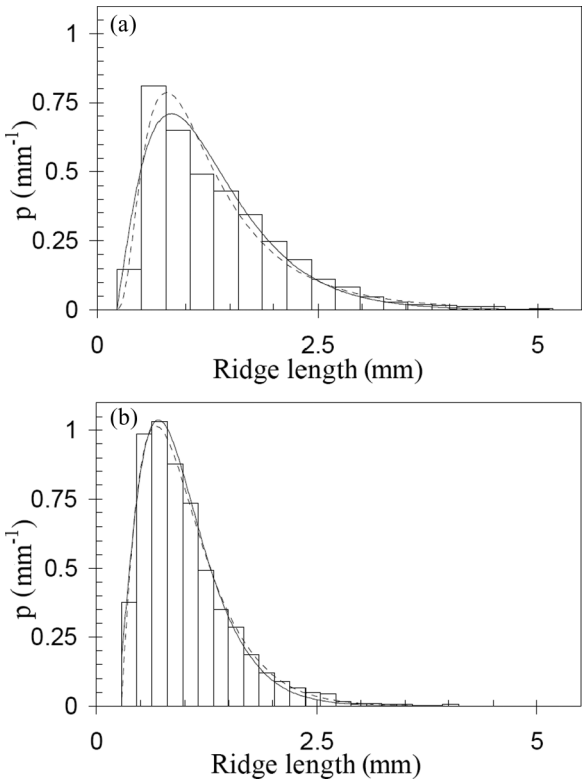

FIG. 3. Statistical distributions of ridge length in a crumpling network formed in hand crushed paper of edge size $L = 100$ mm and thickness $h = 0.068$ mm with the packing densities (a) $\rho = 0.072$ ($R = 26.3$ mm) and (b) $\rho = 0.295$ ($R = 16.4$ mm). Bins: experimental data from Ref. [17] (notice the misprint in Fig. 8 of Ref. [17], where the ridge length is actually measured in pixels); curves: data fittings by (a) log-normal distribution (dashed curve: shift 0.179 mm, scale parameter 1.19 mm, and shape parameter 0.88) and by Eq. (23) with $l_{\min} = 0.204$ mm, $l_{\max} = 6$ mm, $\beta^{-1} = 0.446$ mm, and $D = 2.42$ (solid curve); (b) gamma distribution (dashed curve: shift 0.28 mm, $\beta^{-1} = 0.338$ mm and $D = 2.18$) and by Eq. (23) with $l_{\min} = 0.204$ mm, $l_{\max} = 4.1$ mm, $\beta^{-1} = 0.273$ mm, and $D = 2.82$ (solid curve).

gamma distribution commonly used to fit the experimental data for ridge lengths distribution. In this regard, although the distribution (23) is experimentally indistinguishable from a conventional gamma distribution when $\beta l_{\max} = a > 10$, while $\beta l_{\min} < 0.1$ (see Fig. 4), we found that distribution (24) provides the best fit to available data for experimental crumpling length sets with $\beta l_{\max} = a < 5$ (e.g., see Fig. 3).

B. Thermodynamic potentials of a crumpling network

The elastic energy stored in the crumpling network is equal to $E = \sum_i^N \varepsilon_i$, where ε_i is the elastic energy (6) stored in a single ridge of length l_i [6]. Accordingly, in the thermodynamic limit of $\overline{N} \to \infty$,

$$E = \overline{N} \int dl \varepsilon(l) p(l) = \kappa \overline{N} \int_{l_{\min}}^{l_{\max}} (l/h)^{2/3} p(l) dl = \overline{N} \langle \varepsilon \rangle , \tag{28}$$

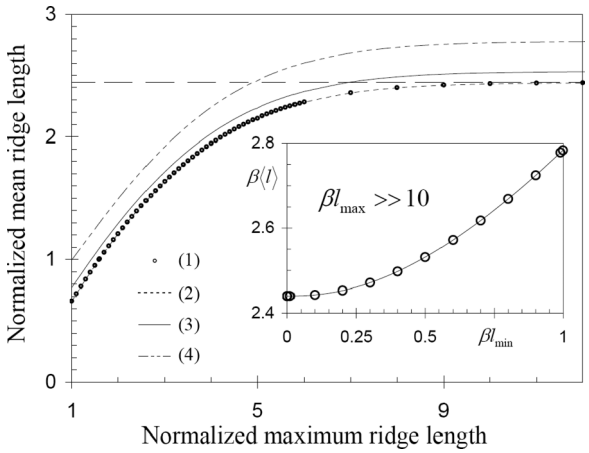

FIG. 4. Normalized mean ridge length $\beta\langle l\rangle$ versus $\beta l_{\max}$ for different $\beta l_{\min} = 0.0001$ (1), 0.1 (2), 0.5 (3), 0.99 (4). Inset shows $\beta\langle l\rangle$ versus $\beta l_{\min}$ for $\beta l_{\max} \gg 1$.

where $\varepsilon(l)$ is given by Eq. (6) and the distribution function $p(l)$ and number of ridges $\overline{N}(\rho)$ are defined by Eqs. (23) and (9), respectively.

Within the Edwards's approach (see Refs. [42–44]), an infinitesimal change of configurational entropy $S(\overline{N}, E, V) = \overline{N} s(\varepsilon, v)$ between two jammed states of the crumpling network can be presented in the form $dS = T_{\text{conf}}^{-1}(dE - \mu d\overline{N}) + X^{-1} dV$, such that

$$ds = T_{\text{conf}}^{-1}(d\varepsilon - \langle \varepsilon \rangle \overline{N}^{-1} d\overline{N}) + X^{-1} dv, \tag{29}$$

where $v = V/\overline{N}$, $V = L^2 h \rho^{-1}$ is the volume of the crumpled ball, and

$$\mu = (\partial E/\partial \overline{N})_{V,S} = \langle \varepsilon \rangle \tag{30}$$

is the chemical potential of the crumpling network, whereas

$$T_{\text{conf}}^{-1} = (\partial s/\partial \varepsilon)_{V,N} \quad \text{and} \quad X^{-1} = (\partial s/\partial v)_{E,N}, \tag{31}$$

are the configurational temperature and compactivity, respectively (see Refs. [43]), while $s(\beta) = -\int_{l_{\min}}^{l_{\max}} p(l) \ln[p(l)] dl + \int_{l_{\min}}^{l_{\max}} p(l) s(l) dl$ and $\beta(v)$ is defined by Eq. (24). Using the distribution function (23), it is a straightforward exercise to derive the expression

$$s(\beta) = 1 + \frac{\gamma(D+1; \beta l_{\min}, a)}{\gamma(D; \beta l_{\min}, a)} + \ln\left[\frac{V_D}{2[N!]^{1/N}} \gamma(D; \beta l_{\min}, a)\right], \tag{32}$$

where

$$\beta^{-1} = (\partial \langle l \rangle / \partial s) = (\partial \varepsilon / \partial \langle l \rangle)^{-1} T_{\text{conf}}, \tag{33}$$

whereas $\zeta = T_{\text{conf}}^{-1} \mu$ and the analog of the Helmholtz free energy of the crumpling network is $F = E - T_{\text{conf}} S$, such that $S(\beta) = \beta^2 (\partial F/\partial \beta)_{\zeta,E}$. In this way, all thermodynamic potentials of the crumpling network can be defined within the framework of Edwards's statistical mechanics.

IV. PRESSURE-PACKING DENSITY RELATIONSHIP

Generally, the mechanical behavior of a randomly crumpled sheet on external loads is governed by the crumpling network response on changes of number of ridges, network volume, and shape. In particular, the crumpling network responses to shear or axial compression are controlled by the shape dependence of the configurational entropy [17], whereas the mechanical behavior of a randomly folded sheet in a three-dimensional stress state is dominated by the volume dependence of elastic energy stored in the network [22], at least in the range (2) of packing density variation. However, as the packing density increases, the entropic contribution to the sheet resistance to hydrostatic pressure can become relevant. It is a straightforward matter to derive the relation between the sheet packing density $\rho = L^2 h/V$ and hydrostatic pressure

$$P = -\left(\frac{\partial E}{\partial V}\right)_{S,N} + \langle \varepsilon \rangle \left(\frac{\partial N}{\partial V}\right)_{E,S} + T_{\text{conf}} \left(\frac{\partial S}{\partial V}\right)_{E,N}. \quad (34)$$

Accordingly, using Eqs. (9), (28), (32), and (33), and taking into account that asymptotically $P \to \infty$ as $\rho \to 1$, the pressure-packing density relationship can be presented in the following form:

$$P = A\rho^{\eta} \left\{ 1 + \frac{(a)^D \exp(-a)}{3\gamma\,(D; a\rho^{\varphi}, a)} \right\}, \quad (35)$$

where the scaling exponent η is equal to

$$\eta = \alpha - \varphi/3 + 1, \quad (36)$$

such that for purely elastic self-avoiding sheets crumpled into balls ($\alpha = 11/9$ and $\varphi = 2/3$) the scaling exponent $\eta = 2$ coincides with the result of numerical simulations in Ref. [28], whereas the material-dependent constant A coincides with that in Eq. (2).

Notice that the first term on the right-hand side of Eq. (35) accounts for the change of number of ridges and total elastic energy stored in the crumpling network, whereas the second term accounts for the change in the network entropy. Accordingly, from graphs in Fig. 5 one can see that as long as the packing density is in the range of Eq. (3), the sheet compressibility is governed by an increase of elastic energy and $P(\rho)$ obeys Eq. (2). For larger packing densities, the entropic contribution becomes relevant and then it becomes dominant as $\rho \to 1$. Figure 6 shows the normalized pressure-packing density curves for an elastic sheet ($D = 22/9$, $\varphi = 2/3$, $\eta = 2$) with different ratio $l_{\max}/l_{\text{mod}} = a/(D-1)$. Notice that as the ratio $l_{\max}/l_{\text{mod}}$ increases, the interval (3) of power-law behavior (2) increases, but the deviation from the power-law at higher packing densities becomes more abrupt, as was observed in numerical simulations reported in Ref. [39].

Plastic deformations of elastoplastic sheets lead to increase of φ [22] and η [14,22,31,38]. In this regard, it should be emphasized that the parameter $a = (D-1)l_{\max}/l_{\text{mod}}$ and scaling exponent $\varphi = \alpha/D_2$ can be determined from studies of crumpling networks. Specifically, these parameters can be obtained from the tomographic [25], or electron microscopy [28] studies of crumpled sheets. Furthermore, such parameters as $l_{\max}$, l_{mod}, D_2, α, and φ can be determined in studies of crumpling network impressions on unfolded sheets (see Refs. [21,22,48,50,55]). So, the master curve P/A versus ρ can be calculated without any mechanical measurement. This may be very useful especially for studies of crumpled nanosheets, e.g., as performed in Ref. [28].

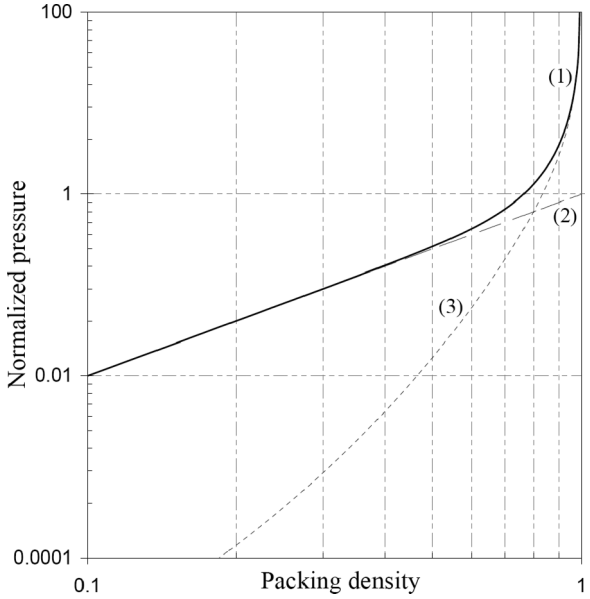

FIG. 5. Log-log plots of normalized pressure (P/A) versus packing density (1) along with the energetic (2) and entropic (3) contributions into $P(\rho)$ behavior (35) for an elastic self-avoiding sheet with $a = 5.2$ ($D = 22/9$ and $\varphi = 2/3$).

On the other hand, in practice, Eqs. (35) and (36) can be used to fit experimental data available in the range (3) and then extrapolate them to higher pressures and larger packing densities. Figure 7 illustrates that Eq. (35) provides an excellent fit of experimental pressure-packing density curve for the aluminum foil crumpled under hydrostatic compression [38].

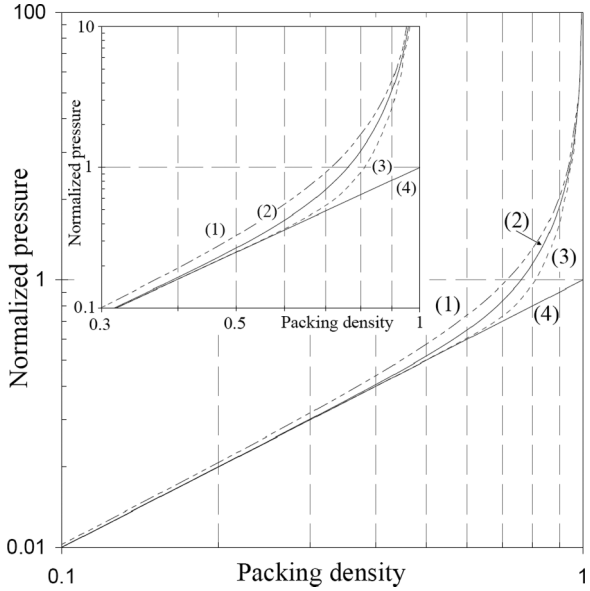

FIG. 6. Log-log plots of normalized pressure (P/A) versus packing density (ρ) for purely elastic sheets with different ratios $l_{\max}/l_{\text{mod}} = 3.37\,(1)$, $8.47\,(2)$, and $15.25\,(3)$; the straight line (4) shows the power-law behavior of Eq. (2). Inset amplifies the deviation of $P(\rho)$ curve from the power law.

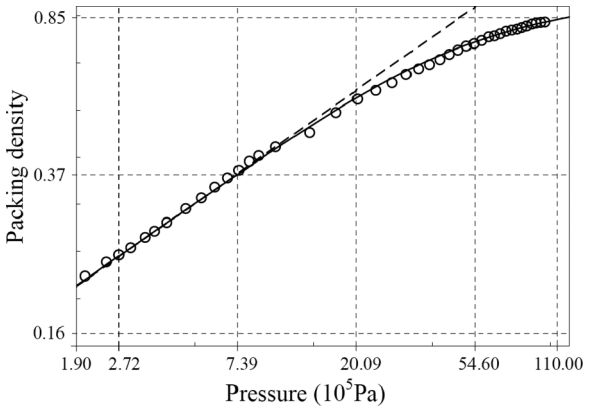

FIG. 7. Log-log plot of packing density (1) versus pressure for the aluminum sheet of thickness $h = 0.016$ mm and edge size $L = 150$ mm. Circles: experimental data from Fig. 2 of Ref. [38], dashed line: power-law asymptotic (2), and solid curve is calculated by Eqs. (35) and (36) with $A = 6.776$ MPa, $a = 10.08$, (10) $D = 2.64$, and $\varphi = 0.817$. For visual appreciation of the fit quality we use the same scales as in Fig. 2 of Ref. [38].

In this regard, it is also pertinent to point out that in Ref. [38] experimental data for sheets of different sizes made from different elastoplastic materials were collapsed into the same master curve $P/A\rho^{\eta}$ versus ρ [56], so the good quality of data fitting in Fig. 7 permits to assume that the contribution from sheet self-contacts into pressure-packing density behavior can be neglected [57]. Nonetheless, comprehensive molecular dynamics simulations are required to validate the finding of this work.

V. CONCLUSIONS

In summary, we develop the Edwards-like approach to statistical mechanics of crumpling networks in randomly crushed self-avoiding sheets with finite bending rigidity. The ridge length distribution function is derived. It is shown that this distribution provides the best fit to available experimental data for hand crushed papers and is consistent with numerical simulations reported in the literature. For the case of isotropic confinement, the maximum and mean ridge lengths are expressed in terms of sheet dimensions and the confinement ratio. This allows us to establish the pressure-packing density relationship, which elucidates the entropic nature of deviation from the power-law behavior. The effect of plastic deformations on the crumpling mechanics is discussed. It is shown that theoretical relationship $P(\rho)$ is consistent with available results of molecular dynamics simulations and provides an excellent fit to available experimental data in the full range of packing density variation. In this way, it is emphasized that all fitting parameters of the pressure packing can be determined by the study of crumpling networks on unfolded elastoplastic sheets. These findings provide further insight into the physics of crumpling and mechanical properties of crumpled soft matter. So, we expect that this paper will stimulate experimental research and numerical simulations of crumpling phenomena.

ACKNOWLEDGMENT

This work was supported by the PEMEX under the SENER-CONACYT research Grant No. 143927.

[1] S. W. Cranford and M. J. Buehler, Packing efficiency and accessible surface area of crumpled graphene, Phys. Rev B **84**, 205451 (2011).

[2] A. Ord and B. Hobbs, Localised folding in general deformations, Tectonophysics **587**, 30 (2013).

[3] A. J. Wood, Witten's lectures on crumpling, Physica A **313**, 83 (2002).

[4] T. A. Witten, How soft matter correlates: three examples, J. Phys.: Condens. Matter **17**, S1651 (2005); Stress focusing in elastic sheets, Rev. Mod. Phys. **79**, 643 (2007).

[5] S. Mao, Z. Wen, H. Kim, G. Lu, P. Hurley, and J. Chen, A general approach to one-pot fabrication of crumpled graphene-based nanohybrids for energy applications, ACS Nano **6**, 7505 (2012); C. N. Lau, W. Bao, and J. Velasco, Properties of suspended graphene membranes, Mater. Today **15**, 238 (2012); X. Ma, M. R. Zachariah, and C. D. Zangmeister, Reduction of suspended graphene oxide single sheet nanopaper: the effect of crumpling, J. Phys. Chem. C **117**, 3185 (2013); O. Bouaziz, J. P. Masse, S. Allain, L. Orgéas, and P. Latil, Compression of crumpled aluminum thin foils and comparison with other cellular materials, Mater. Sci. Eng. A **570**, 1 (2013); R. Kempaiaha and Z. Nie, From nature to synthetic systems: shape transformation in soft materials, J. Mater. Chem. B **2**, 2357 (2014).

[6] A. Lobkovsky, S. Gentges, H. Li, D. Morse, and T. A. Witten, Scaling properties of stretching ridges in a crumpled elastic sheet, Science **270**, 1482 (1995); A. E. Lobkovsky and T. A. Witten, Properties of ridges in elastic membranes, Phys. Rev. E **55**, 1577 (1997).

[7] E. Cerda, S. Chaieb, F. Melo, and L. Mahadevan, Conical dislocations in crumpling, Nature **401**, 46 (1999); B. A. DiDonna, T. A. Witten, S. C. Venkataramani, and E. M. Kramer, Singularities, structures, and scaling in deformed m-dimensional elastic manifolds, Phys. Rev. E **65**, 016603 (2001); T. Liang and T. A. Witten, Crescent singularities in crumpled sheets, *ibid.* **71**, 016612 (2005).

[8] R. D. Schroll, E. Katifori, and B. Davidovitch, Elastic building blocks for confined sheets, Phys. Rev. Lett. **106**, 074301 (2011).

[9] E. M. Kramer and T. A. Witten, Stress condensation in crushed elastic manifolds, Phys. Rev. Lett. **78**, 1303 (1997).

[10] B. A. DiDonna and T. A. Witten, Anomalous strength of membranes with elastic ridges, Phys. Rev. Lett. **87**, 206105 (2001).

[11] J. A. Åström, J. Timonen, and M. Karttunen, Crumpling of a stiff tethered membrane, Phys. Rev. Lett. **93**, 244301 (2004).

[12] K. Matan, R. B. Williams, T. A. Witten, and S. R. Nagel, Crumpling a thin sheet, Phys. Rev. Lett. **88**, 076101 (2002).

[13] A. S. Balankin, I. Campos Silva, O. A. Martínez, and O. Susarrey Huerta, Scaling properties of randomly folded plastic sheets, Phys. Rev. E **75**, 051117 (2007).

[14] Y. C. Lin, Y. L. Wang, Y. Liu, and T. M. Hong, Crumpling under an ambient pressure, Phys. Rev. Lett. **101**, 125504 (2008).

[15] S. Deboeuf, E. Katzav, A. Boudaoud, D. Bonn, and M. Adda-Bedia, Comparative study of crumpling and folding of thin sheets, Phys. Rev. Lett. **110**, 104301 (2013).

[16] A. S. Balankin, D. Samayoa Ochoa, E. Pineda León, R. C. Montes de Oca, A. Horta Rangel, and M. A. Martínez Cruz, Power law scaling of lateral deformations with universal Poisson's index for randomly folded thin sheets, Phys. Rev. B **77**, 125421 (2008).

[17] A. S. Balankin and O. Susarrey Huerta, Entropic rigidity of a crumpling network in a randomly folded thin sheet, Phys. Rev. E **77**, 051124 (2008).

[18] A. S. Balankin, O. Susarrey Huerta, F. Hernández Méndez, and J. Patiño Ortiz, Slow dynamics of stress and strain relaxation in randomly crumpled elastoplastic sheets, Phys. Rev. E **84**, 021118 (2011).

[19] A. S. Balankin, O. Susarrey Huerta, and V. Tapia, Statistics of energy dissipation and stress relaxation in a crumpling network of randomly folded aluminum foils, Phys. Rev. E **88**, 032402 (2013).

[20] C. Hui, Y. Zhang, L. Zhang, R. Sun, and F. Liu, Crumpling of a pyrolytic graphite sheet, J. Appl. Phys. **114**, 163512 (2013).

[21] A. S. Balankin, O. Susarrey Huerta, R. C. M. de Oca, D. S. Ochoa, J. M. Trinidad, and M. A. Mendoza, Intrinsically anomalous roughness of randomly crumpled thin sheets, Phys. Rev. E **74**, 061602 (2006).

[22] A. S. Balankin, A. H. Rangel, G. G. Pérez, F. G. Martinez, H. S. Chavez, and C. L. Martínez-González, Fractal features of a crumpling network in randomly folded thin matter and mechanics of sheet crushing, Phys. Rev. E **87**, 052806 (2013).

[23] A. S. Balankin, R. C. M. de Oca, and D. S. Ochoa, Intrinsically anomalous self-similarity of randomly folded matter, Phys. Rev. E **76**, 032101 (2007).

[24] A. S. Balankin, D. S. Ochoa, I. A. Miguel, J. P. Ortiz, and M. A. M. Cruz, Fractal topology of hand-crumpled paper, Phys. Rev. E **81**, 061126 (2010).

[25] Y.-C. Lin, J.-M. Sun, H. W. Yang, Y. Hwu, C. L. Wang, and T.-M. Hong, X-ray tomography of a crumpled plastoelastic thin sheet, Phys. Rev. E **80**, 066114 (2009).

[26] Y.-C. Lin, J.-M. Sun, J.-H. Hsiao, Y. Hwu, C. L. Wang, and T.-M. Hong, Spontaneous emergence of ordered phases in crumpled sheets, Phys. Rev. Lett. **103**, 263902 (2009).

[27] M. A. F. Gomes, Fractal geometry in crumpled paper balls, Am. J. Phys. **55**, 649 (1987); Paper crushes fractally, J. Phys. A: Math. Gen. **20**, L283 (1987); R. Cassia-Moura and M. A. F. Gomes, A crumpled surface having transverse attractive interactions as a simplified model with biological significance, J. Theor. Biol. **238**, 331 (2006); M. A. F. Gomes, C. C. Donato, S. L. Campello, R. E. de Souza, and R. Cassia-Moura, Structural properties of crumpled cream layers, J. Phys. D: Appl. Phys. **40**, 3665 (2007).

[28] X. Ma, M. R. Zachariah, and C. D. Zangmeister, Crumpled nanopaper from graphene oxide, Nano Lett. **12**, 486 (2012); W.-N. Wang, Y. Jiang, and P. Biswas, Evaporation-induced crumpling of graphene oxide nanosheets in aerosolized droplets: confinement force relationship, J. Phys. Chem. Lett. **3**, 3228 (2012).

[29] G. A. Vliegenthart and G. Gompper, Forced crumpling of self-avoiding elastic sheets, Nat. Mater. **5**, 216 (2006).

[30] T. Tallinen, J. A. Åström, and J. Timonen, Deterministic folding in stiff elastic membranes, Phys. Rev. Lett. **101**, 106101 (2008); T. Tallinen, J. A. Aström, and J. Timonen, Discrete element simulations of crumpling of thin sheets, Comput. Phys. Commun. **180**, 512 (2009).

[31] T. Tallinen, J. A. Åström, and J. Timonen, The effect of plasticity in crumpling of thin sheets, Nat. Mater. **8**, 25 (2009).

[32] M. A. F. Gomes and V. M. Oliveira, Repacking of crumpled systems, Philos. Mag. Lett. **78**, 325 (1998).

[33] R. S. Mendes, L. C. Malacarne, R. P. B. Santos, H. V. Ribeiro, and S. Picoli, Earthquake-like patterns of acoustic emission in crumpled plastic sheets, Europhys. Lett. **92**, 29001 (2010).

[34] A. S. Balankin, D. M. Matamoros, E. P. León, A. H. Rangel, M. A. M. Cruz, and D. S. Ochoa, Topological crossovers in the forced folding of self-avoiding matter, Phys. A **388**, 1780, (2009).

[35] L. Bevilacqua, Fractal balls, Appl. Math. Model. **28**, 547 (2004).

[36] T. Tallinen, J. A. Åström, P. Kekäläinen, and J. Timonen, Mechanical and thermal stability of adhesive membranes with nonzero bending rigidity, Phys. Rev. Lett. **105**, 026103 (2010).

[37] Sh.-F. Liou, Ch.-Ch. Lo, M.-H. Chou, P.-Y. Hsiao, and T.-M. Hon, Effect of ridge-ridge interactions in crumpled thin sheets, Phys. Rev. E **89**, 022404 (2014).

[38] W. Bai, Y.-C. Lin, T.-K. Hou, and T.-M. Hong, Scaling relation for a compact crumpled thin sheet, Phys. Rev. E **82**, 066112 (2010).

[39] C. Chang, Z. Song, J. Lin, and Z. Xu, How graphene crumples are stabilized? RSC Adv. **3**, 2720 (2013).

[40] H. Aharoni and E. Sharon, Direct observation of the temporal and spatial dynamics during crumpling, Nat. Mater. **9**, 993 (2010).

[41] M. Adda-Bedia, A. Boudaoud, L. Boué, and S. Deboeuf, Statistical distributions in the folding of elastic structures, J. Stat. Mech. Theor. Exp. (2010) P11027.

[42] M. P. Ciamarra, P. Richard, M. Schröter, and B. P. Tighe, Statistical mechanics for static granular media: open questions, Soft Matter **8**, 9731 (2012).

[43] S. F. Edwards and R. B. S. Oakeshott, Theory of powders, Phys. A **157**, 1080 (1989); S. F. Edwards, D. V. Grinev, and J. Brujić, Fundamental problems in statistical physics of jammed packings, *ibid.* **330**, 61 (2003); S. F. Edwards, New kinds of entropy, J. Stat. Phys. **116**, 29 (2004); R. Blumenfeld and S. F. Edwards, Granular entropy: explicit calculations for planar assemblies, Phys. Rev. Lett. **90**, 114303 (2003); T. Aste, T. Di Matteo, M. Saadatfar, T. J. Senden, M. Schröter, and H. L. Swinney, An invariant distribution in static granular media, Europhys. Lett. **79**, 24003 (2006); C. Briscoe, C. Song, P. Wang, and H. A. Makse, Entropy of jammed matter, Phys. Rev. Lett. **101**, 188001 (2008); J. G. Puckett and K. E. Daniels, Equilibrating temperaturelike variables in jammed granular subsystems, *ibid.* **110**, 058001 (2013).

[44] R. Blumenfeld and S. F. Edwards, Geometric partition functions of cellular systems: Explicit calculation of the entropy in two and three dimensions, Eur. Phys. J. E **19**, 23 (2006).

[45] L. D. Landau and E. M. Lifshitz, *Theory of Elasticity* (Pergamon, Oxford, 1986).
[46] A. E. Lobkovsky, Boundary layer analysis of the ridge singularity in a thin plate, Phys. Rev. E **53**, 3750 (1996).
[47] H. Bermúdez, D. A. Hammer, and D. E. Discher, Effect of bilayer thickness on membrane bending rigidity, Langmuir **20**, 540 (2004).
[48] D. L. Blair and A. Kudrolli, Geometry of crumpled paper, Phys. Rev. Lett. **94**, 166107 (2005).
[49] E. Sultan and A. Boudaoud, Statistics of crumpled paper, Phys. Rev. Lett. **96**, 136103 (2006).
[50] C. A. Andresen, A. Hansen, and J. Schmittbuhl, Ridge network in crumpled paper, Phys. Rev. E **76**, 026108 (2007).
[51] S. Deboeuf, M. Adda-Bedia, and A. Boudaoud, Energy distributions and effective temperatures in the packing of elastic sheets, Europhys. Lett. **85**, 24002 (2009).
[52] D. Aristoff and C. Radin, Layering in crumpled sheets, Europhys. Lett. **91**, 56003 (2010).
[53] I. Dierking and P. Archer, Sudden ridge collapse in the stress relaxation of thin crumpled polymer films, Phys. Rev. E **77**, 051608 (2008).
[54] V. E. Tarasov, *Fractional Dynamics, Nonlinear Physical Science* (Springer, Berlin, 2010).
[55] C.-T. Hsu and M. Huang, Ridge network detection in crumpled paper via graph density maximization, IEEE Trans. Image Process. **21**, 4498 (2012).
[56] It is easy to understand that graphs from Fig. 1 of Ref. [37], Figs. 2(a) and 2(b) of Ref. [39], and Figs. 4–6 of Ref. [38] can be reproduced with Eq. (35). Unfortunately, the low resolution of these graphs and the needs of coordinate transformations result in a very larger uncertainty, such that the comparison with theoretical curves (35) cannot be treated in a quantitative way.
[57] In fact, it is reasonable to expect that the contribution from sheet self-contacts increases as a power law of the packing density, whereas the entropic contribution is an almost exponential function of ρ.